J. exp. Biol. **116**, 79–107 (1985)
Printed in Great Britain © *The Company of Biologists Limited 1985*

FLIGHT MECHANICS OF A DRAGONFLY

BY AKIRA AZUMA, SOICHI AZUMA, ISAO WATANABE AND TOYOHIKO FURUTA

Institute of Interdisciplinary Research, Faculty of Engineering, The University of Tokyo, Tokyo, Japan

Accepted 6 September 1984

SUMMARY

The steady slow climbing flight of a dragonfly, *Sympetrum frequens*, was filmed and analysed. By using the observed data, the mechanical characteristics of the beating wings were carefully analysed by a simple method based on the momentum theory and the blade element theory, and with a numerical method modified from the local circulation method (LCM), which has been developed for analysing the aerodynamic characteristics of rotary wings.

The results of calculations based on the observed data show that the dragonfly performs low speed flight with ordinary airfoil characteristics, instead of adopting an abnormally large lift coefficient. The observed phase advance of the hindwing, $\Delta\delta_1 \simeq 80°$ can be fully explained by the present theoretical calculation. Similarly, the spanwise variation of the airloading and the time variations of the horizontal force, vertical force, pitching moment and torque or power can be definitely estimated within a reasonable range of accuracy in comparison with the flight data. The distribution of loading between the fore and hind pairs of wings is also clarified by the calculations.

INTRODUCTION

Dragonflies (Order Odonata) are excellent flyers and are characterized by a large head – much of which is occupied by huge eyes and a relatively large mouth – a robust thorax, two pairs of almost identically shaped wings, and a large, long, slender abdomen. Dragonflies can hover, fly at high speed and manoeuvre skilfully in the air in order to defend their territory, feed on live prey and mate in tandem formation.

The biology of dragonflies has been closely studied but few attempts have been made to analyse their flight mechanics. Norberg (1975) filmed the free hovering flight of *Aeschna juncea* in the field and found that the body is held almost horizontal and that both the fore and hind pairs of wings are beaten at a frequency of 36 Hz in two stroke planes which are almost parallel and tilted 60° relative to the horizontal.

Key words: Flight, dragonfly, mechanics.

Weis-Fogh (1972), in his analysis of hovering flight, assumed (1) a constant induced velocity distribution over the stroke plane (based on the momentum theory), (2) a simple harmonic motion of the beating wings, and (3) a constant pitch along the span of the wing. Then, following the techniques used in the analysis of helicopter rotor aerodynamics (Gessow & Myers, 1952), he carried out a steady aerodynamic calculation on the beating wings by integrating the elemental forces acting on a blade element over the wings with the aid of strip analysis and by averaging these forces over one stroke cycle. The results required abnormally large lift coefficients, of 3·5 to 6·1.

In order to get a more realistic model of the flow field around the beating wings, Rayner (1979*a,b,c*) introduced the vortex theory for a pair of wings, in which a chain of coaxial, small-cored, circular vortex rings, simulating the trailing tip-vortices of wings, was brought into the calculation of the induced velocity, as had been developed for rotary wing aerodynamics (Heyson & Katzoff, 1957). However, unlike a helicopter rotor in hovering flight, two pairs of wings arranged in tandem have time-varying airloadings and thus, as shown in Fig. 1, generate two corrugated wake sheets filled respectively with a sheet of shed vortices as well as trailing vortices. Thus, the induced velocity, which, unlike that of the hovering rotor, is not always vertical, must be estimated from both the trailing and shed vortices. The wake of the vortices is of considerable importance in and near hovering flight because the downwash generated by a wing, which is retained and developed from the stroke plane, strongly affects the angle of attack of the wing in the subsequent stroke and of another wing operating nearby.

In the case of a helicopter rotor, such effects of the downwash on the airloadings of the succeeding wing have been accurately analysed by simply introducing an attenuation coefficient instead of performing the complex integration over the vortex sheet (Azuma & Kawachi, 1979). This method of calculation, called the 'Local Momentum Theory' (LMT), has been extended to the study of the unsteady aerodynamics in the rotary wing of a helicopter (Azuma & Saito, 1982) and also, under the name of the 'Local Circulation Method' (LCM), to analyses of the highly skewed flow of propellers (Azuma, Nasu & Hayashi, 1981) and the windmill (Azuma, Hayashi & Ito, 1982).

Since the fundamental aerodynamic characteristics of the beating wing are much like those of the rotary wing, even though wing beating is a reciprocating motion and not a rotational motion like that of a rotary wing, the LCM can similarly be applied to the aerodynamic analysis of the beating wing with a slight modification of the method.

SYMBOLS

a	vector quantity defined by equation (36),
C_λ	lift coefficient,
C_d	drag coefficient,
C_{hf}, C_{fh}	interference coefficients between fore- and hindwings defined by equations (30),

C_h^j, C_f^j	attenuation coefficients defined by equation (31),
c	wing chord,
D	drag,
F	force,
I	moment of inertia of a wing about a flapping hinge,
i, j	running variables,
k	reduced frequency = $\omega c/2U$,
L	lift,
l	lift of wing element in vectorial form,
λ	airloading = $\|l\|$,
M	pitching moment,
m	mass of wing,

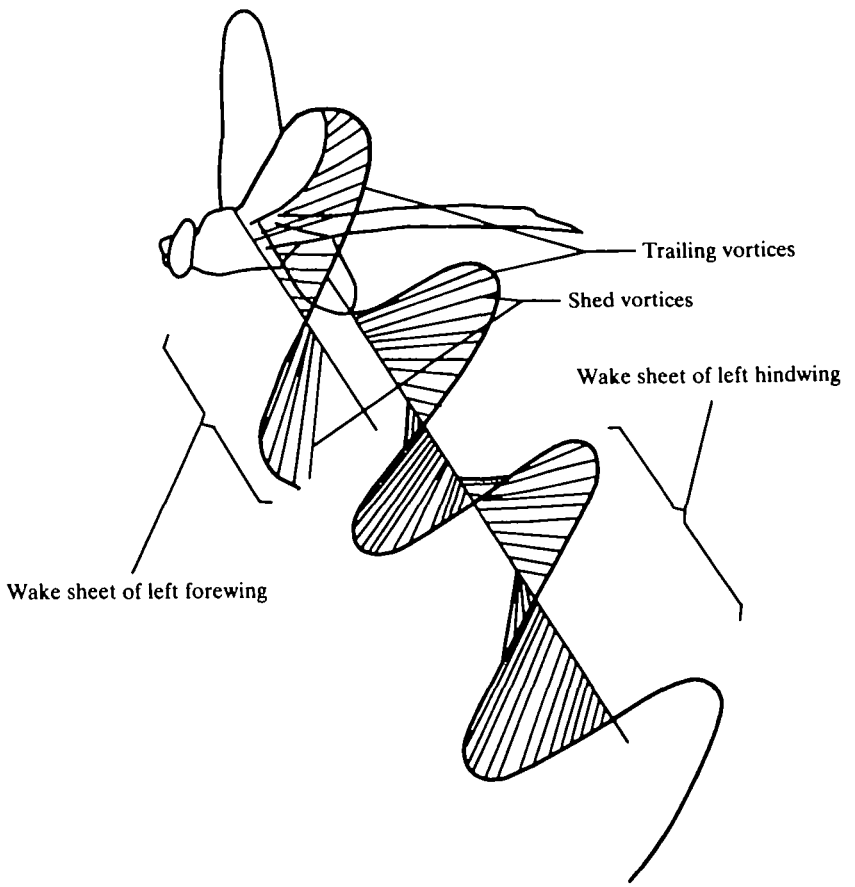

Fig. 1. Wake model of beating wings. Wake sheets of left wings are shown.

n	n-th harmonic; running variable,
P	power,
Q	torque,
R	radius of wing or half span of wing pair,
Re	Reynolds number,
ν	vectorial position of a vortex element,
r	radial or spanwise position,
(r, ψ, ζ)	polar coordinate system,
S	area of stroke plane,
S_e	swept area of stroke plane,
s	spanwise unit vector,
T	thrust,
t	time,
U	total velocity of wing element in vectorial form,
U	total inflow velocity of wing element, $U = \|U\|$,
V	forward velocity,
v	induced velocity,
W	weight,
(X, Y, Z)	coordinate axes fixed in inertial space,
(x, y, z)	local coordinate axes,
x	non-dimensional spanwise position $= r/R$,
α	angle of attack defined in equations (10),
Γ	circulation,
Δ	small increment; time step,
δ	phase difference of azimuth angle,
ϵ	phase difference of pitch angle,
θ	pitch angle,
π	the circular constant,
ρ	air density,
Σ	summation,
ϕ	inflow angle defined in equations (10),
γ	tilt angle of stroke plane,
ψ	flapping or azimuth angle,
ω	angular rate of flapping motion,

Subscript

a	aerodynamic component,
CG	centre of gravity,
f	fore,
h	hind,
i, j, n	i-th, j-th or n-th quantities,
o	constant; o-th order quantities,
i	inertial component,

P, p, n perpendicular components,
T, q tangential components,
X, Y, Z X, Y and Z components of (X, Y, Z) axes.

Superscript

$(\bar{\ })$ mean value of ( ) defined by equation (16),
$(\dot{\ }), (\ddot{\ })$ time derivatives = $d(\ )/dt$, $d^2(\ )/dt^2$,
j time step.

MODES OF WING MOTION

A dragonfly, *Sympetrum frequens*, flying under a spotlight in a darkened room was filmed with a high speed 16 mm movie camera (HIMAC) at 873 frames per second. The dimensions of the dragonfly are shown in Fig. 2 and Table 1.

In order to get a clear image of the feathering motion of the wings, a 2·5 mm width of each wing tip was painted with 'Pentel White' 03-667-3331EX237 (Fig. 3). The

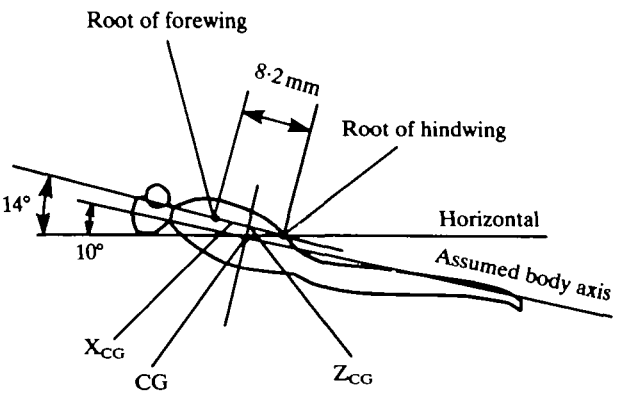

Fig. 2. Diagram of dragonfly, *Sympetrum frequens*. Arrangement of wings and centre of gravity, CG.

Table 1. *Dimensions of the experimental dragonfly*

Parameter		Dimensions	
Length		4·0 cm	4×10^{-2} m
Mass		260 mg	$2{\cdot}60 \times 10^{-4}$ kg
Wing span	forewing	6·7 cm	$6{\cdot}7 \times 10^{-2}$ m
	hindwing	6·5 cm	$6{\cdot}5 \times 10^{-2}$ m
Wing area	forewing	4·42 cm^2	$4{\cdot}42 \times 10^{-4}$ m^2
	hindwing	5·44 cm^2	$5{\cdot}44 \times 10^{-4}$ m^2
Aspect ratio	forewing	10·2	
	hindwing	7·8	
Total wing loading		0·0264 g cm^{-2}	2·58 N m^{-2}
Tilt angle of the wing roots		14°	
Distance of wing roots		8·2 mm	$8{\cdot}2 \times 10^{-3}$ m
Centre of gravity, assumed		$x_{CG} = 7{\cdot}2$ mm	$7{\cdot}2 \times 10^{-3}$ m
		$z_{CG} \simeq 0$	0

mass of the paint was about 0·03 mg, which was about 2 % of the mass of the wing (1·5 mg) and was somewhat less heavy than the pterostigma. The additional moment of inertia caused by the paint about the flapping hinge was $3{\cdot}0 \times 10^{-4}\,\mathrm{gcm}^2$, which was about 5% of that of the wing ($5{\cdot}6 \times 10^{-3}\,\mathrm{gcm}^2$). The additional moment of inertia of the paint about the feathering axis was $2{\cdot}2 \times 10^{-6}\,\mathrm{gcm}^2$, which was about 3·5 % of that of the wing ($6{\cdot}3 \times 10^{-5}\,\mathrm{gcm}^2$). The local backward shift of the centre of mass at the painted portion of the wing was about 4·6 % of the chord.

The mass of paint therefore has a small effect on the beating motion of the wing. However, an experimental check of the beating frequency by means of stroboscope and video camera did not reveal any difference between a painted dragonfly and a naked or unpainted one, although the beating frequency was estimated to be reduced by about 2·5 %. In comparison with Norberg's result (1972) on the inertial effects of the pterostigma on the wing motion it can be considered that the mode of beating was not significantly altered by the painting and the analysed data gave useful information about the flight mechanics of the dragonfly.

Analysis of a series of frames of almost steady flight of the dragonfly in very slow climbing flight revealed the following (Fig. 3).

(i) The body axis, which is a straight line connecting the tip of the head and the tip of the tail, is tipped about 10° head-up with respect to the horizontal.

(ii) The orbit of the wing tips of the hind pair is almost completely in a single plane but the profile of the orbit of the fore pair is a very thin ellipse, the major axis of which may be considered to be the stroke plane. Both stroke planes are tilted about 50° with respect to the body axis, or $\gamma = 40°$ with respect to the horizontal as shown in Fig. 4.

(iii) The beating frequency of all wings is 41·5 Hz.

(iv) The flapping angles or the azimuth angles of the observed data in the respective stroke planes are shown in Fig. 5. The Fourier expansion series of the observed data,

$$\psi = \psi_0 + \sum_{n=1}^{\infty} \psi_n \cos(n\omega t + \delta_n),$$

is well represented by:

$$\left.\begin{aligned} \psi_f &= -3 - 43\cos(\omega t) \\ \psi_h &= 2 - 47\cos(\omega t + 77). \end{aligned}\right\} \text{ (in degrees)} \qquad (1)$$

By comparing this again with the observed data in Fig. 5, the angular speed was found to be $\omega = 2\pi \times 41{\cdot}5\,\mathrm{rad\,s^{-1}} \simeq 15\,000°\,\mathrm{s^{-1}}$ and the phase difference between fore and hind pairs of wings to be $\Delta\delta = \delta_{1,h} - \delta_{1,f} = 77°$, by which the fore pair followed the hind pair.

Fig. 3. A series of frames (time interval = 1·15 ms) showing modes of beating in steady flight of a dragonfly (*Sympetrum frequens*) (wing tips marked with white paint).

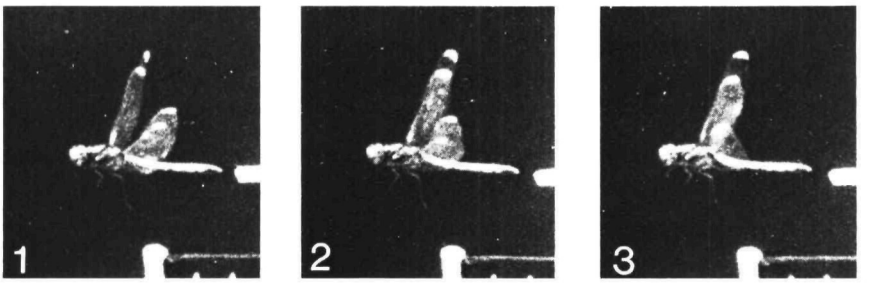

Initiation of the downstroke of the forewings

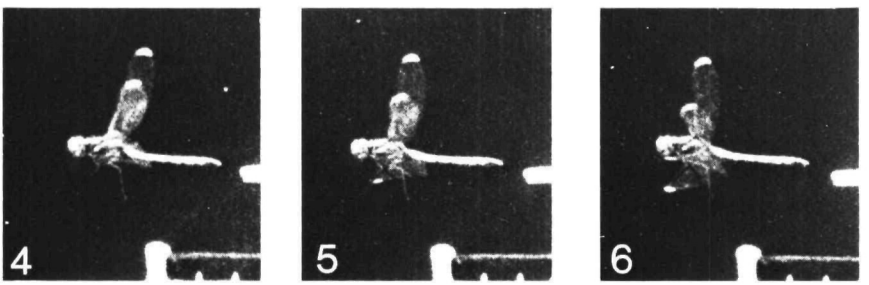

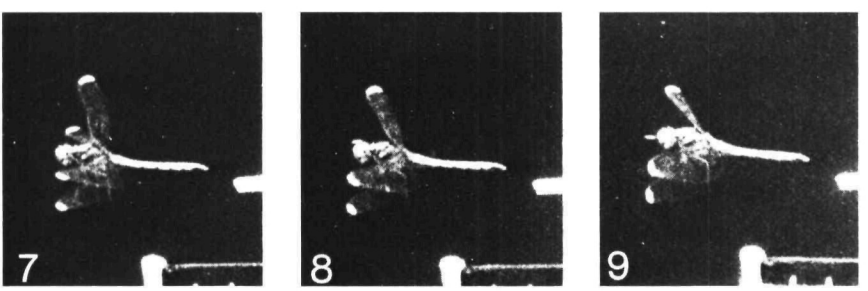

Supination of the hindwings

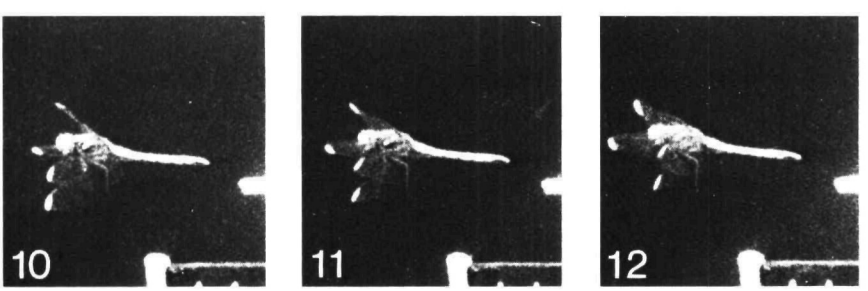

End of the downstroke of the forewings

Supination of the forewings

Fig. 3. 1–12

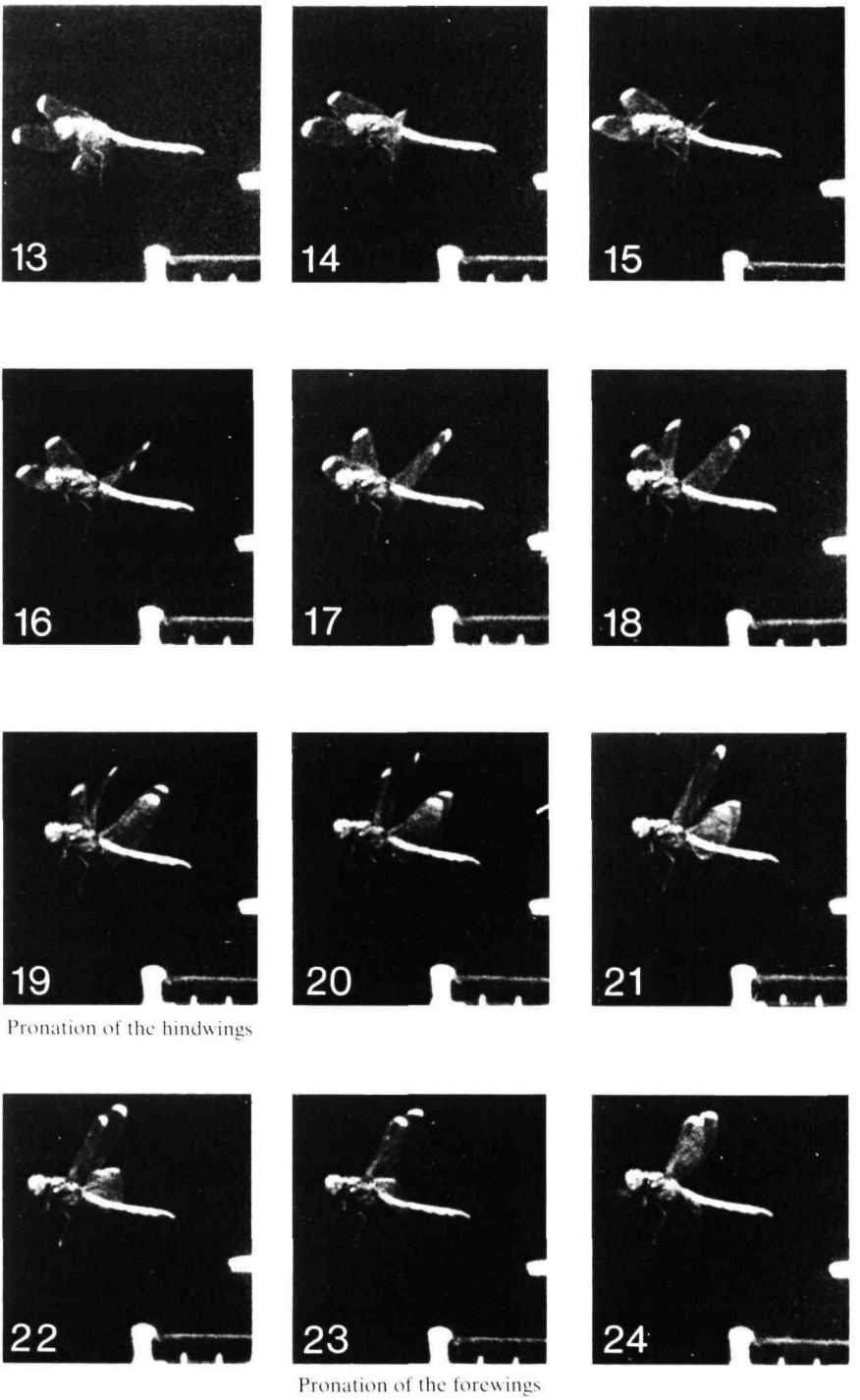
13
14
15
16
17
18
19
20
21
Pronation of the hindwings
22
23
24
Pronation of the forewings

Fig. 3. 13–24

(v) The flight velocity, V, is $0{\cdot}54\,\mathrm{m\,s^{-1}}$, in a direction nearly normal to the stroke plane.

(vi) The pitch variation of the wings with respect to the stroke plane was determined by observing the wing tips, which were marked with white paint as stated before. The Fourier expansion series of the observed data,

$$\theta = \theta_0 + \sum_{n=1}^{\infty} \theta_n \cos(n\omega t + \epsilon_n),$$

is well represented by:

$$\left.\begin{aligned} \theta_f &= 98 - 77\cos(\omega t - 49) - 3\cos(2\omega t + 67) - 8\cos(3\omega t + 29) \\ \theta_h &= 93 - 65\cos(\omega t + 18) + 8\cos(2\omega t + 74) + 8\cos(3\omega t + 28) \end{aligned}\right\} \quad \text{(in degrees)} \quad (2)$$

and shown, with the observed data, in Fig. 6. It is interesting to find that the pitch change consists of a higher (third) harmonic than the flapping stroke which consists of the first harmonic.

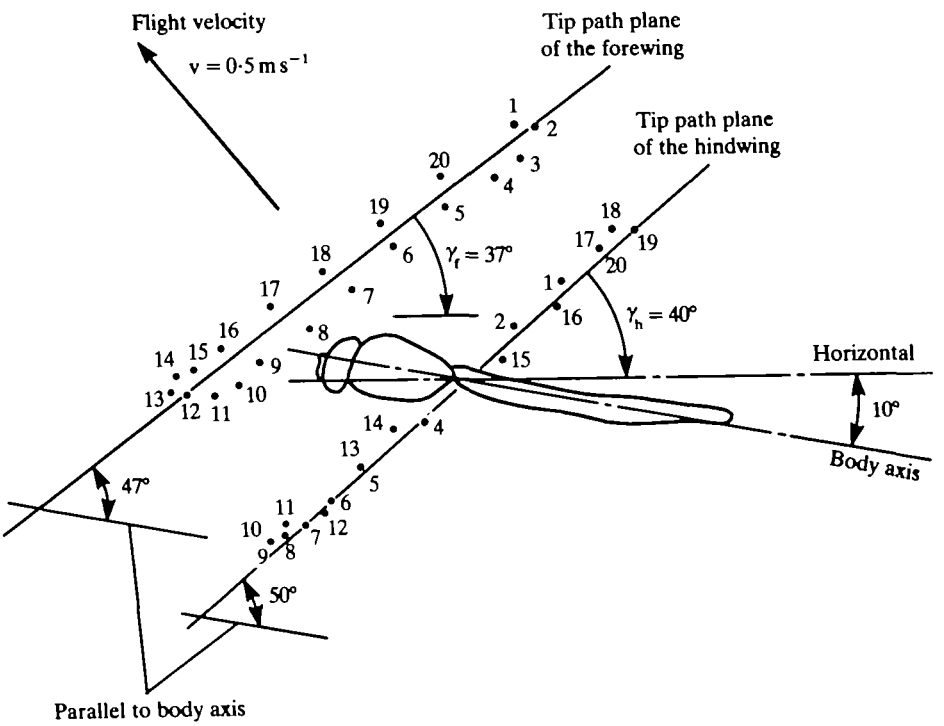

Fig. 4. Orbits of wing tips.

(vii) The maximum values of the Reynolds number and the reduced frequency at three-quarter radius point are $Re = 3{\cdot}2 \times 10^3$ and $k = \omega c/2U = 0{\cdot}12$ respectively.

SIMPLE ANALYSIS

Let us consider the beating motion of a wing (left wing of the fore pair) as shown in Fig. 7. The motion is considered to consist of flapping in the stroke plane about a hinge at the wing root and of feathering about a straight line connected to the aerodynamic centre. By assuming that the wing root is a universal joint located in a symmetrical plane, (X, Z), an element of the wing can be specified by the ordinates of radius r and the azimuth angle ψ in a stroke plane which is tilted by γ with respect to the X-axis directed backward in the horizontal plane. Thus, in order to make an orthogonal Cartesian coordinate system (X, Y, Z), the Y-axis is directed to the right in the horizontal plane and the Z-axis is directed vertically upward. A local coordinate system (x, y, z) is defined as follows. The x-axis or feathering axis is directed outward along the aerodynamic centre or quarter chord line of the wing and is assumed to be

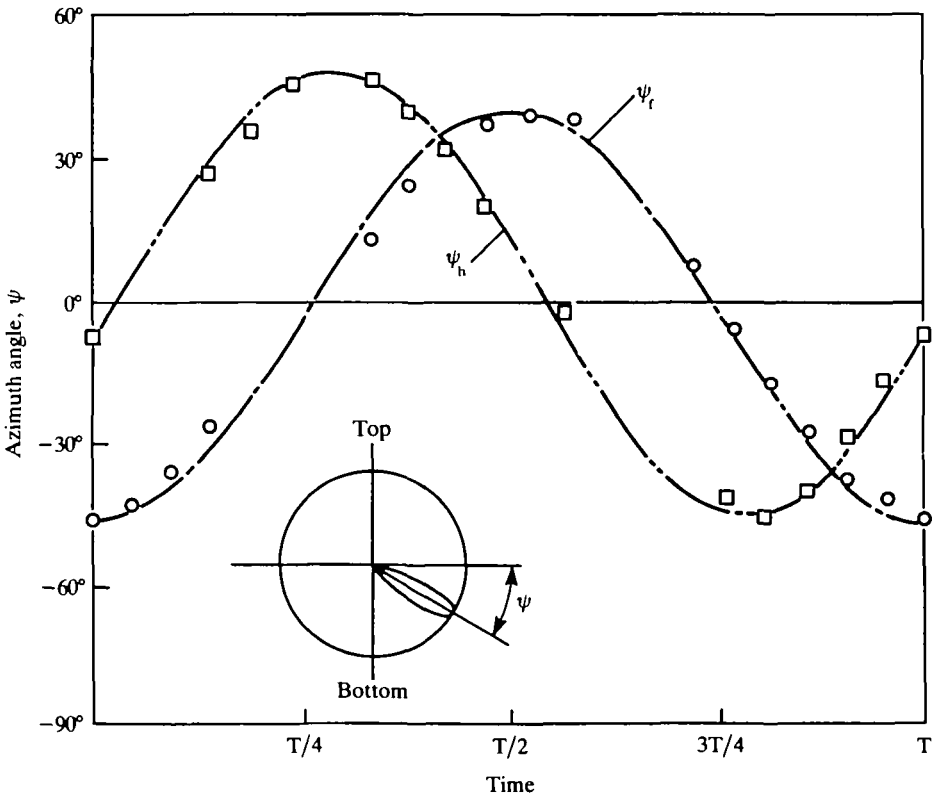

Fig. 5. Trace of azimuth angle. ○, forewings; □, hindwings; observed data.

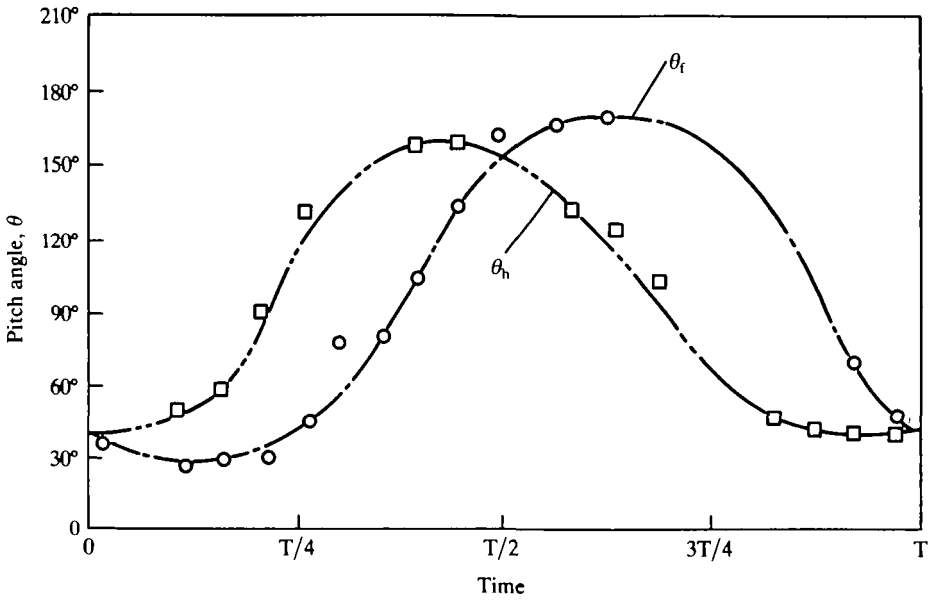

Fig. 6. Pitch variation. ○, forewings; □, hindwings; observed data.

common for all wing sections. The y-axis is directed in the direction of the inflow at the wing section in consideration. The z-axis is directed to make an orthogonal Cartesian coordinate system together with the other two axes. Then the transformation matrix between the (X, Y, Z) axes and the (x, y, z) axes can be given by:

	x	y	z
X	$-\sin\psi\cos\gamma$	$\cos\psi\cos\phi\cos\gamma+\sin\phi\sin\gamma$	$\cos\psi\sin\phi\cos\gamma-\cos\phi\sin\gamma$
Y	$-\cos\psi$	$-\sin\psi\cos\phi$	$-\sin\psi\sin\phi$
Z	$-\sin\psi\sin\gamma$	$\cos\psi\cos\phi\sin\gamma-\sin\phi\cos\gamma$	$\cos\psi\sin\phi\sin\gamma+\cos\phi\cos\gamma$

(3)

In the calculation of the aerodynamic forces, the following assumptions are introduced:

(i) The respective wings sustain a quarter of the total force evenly, $\bar{T}/2$, where $\bar{T}$ is the mean thrust or the mean force generated by the respective pairs of wings and is, because of the negligibly small parasite drag of the body, balanced by the weight:

$$\bar{T} = W/2\cos\gamma. \tag{4}$$

(ii) The pitch angle is independent of the spanwise position $x = r/R$ where R is half of the wing span.

(iii) The induced velocities generated by the fore- and hindwings are constant over and normal to the stroke planes and are determined by the momentum theory as:

$$\left.\begin{aligned} v_f &= -(V/2) + \sqrt{T/2\rho S_e + (V/2)^2} \text{ for forewing} \\ v_h &= -(V + C_{hf}v_f) + \sqrt{T/2\rho S_e + (V + C_{hf}v_f)^2/4}, \text{ for hindwing} \end{aligned}\right\} \quad (5)$$

where S_e is the area swept by one pair of beating wings and C_{hf} is an interference coefficient specifying the effect of the induced velocity of the fore pair on the hind pair, whereas the effect of the hind pair on the fore pair has been neglected because it is so small.

(iv) By neglecting the outflow along the span, the aerodynamic forces acting on a blade element are given by those of two-dimensional airfoils and can be integrated along the span without any interference among the elements.

(v) The aerodynamic characteristics of the wing section or airfoil at low Reynolds number (Fig. 8) were modelled by referring to those given by Vogel (1967) and Jensen (1956), and modified to have the maximum lift coefficient of $C_{L,max} = 1{\cdot}8$ by

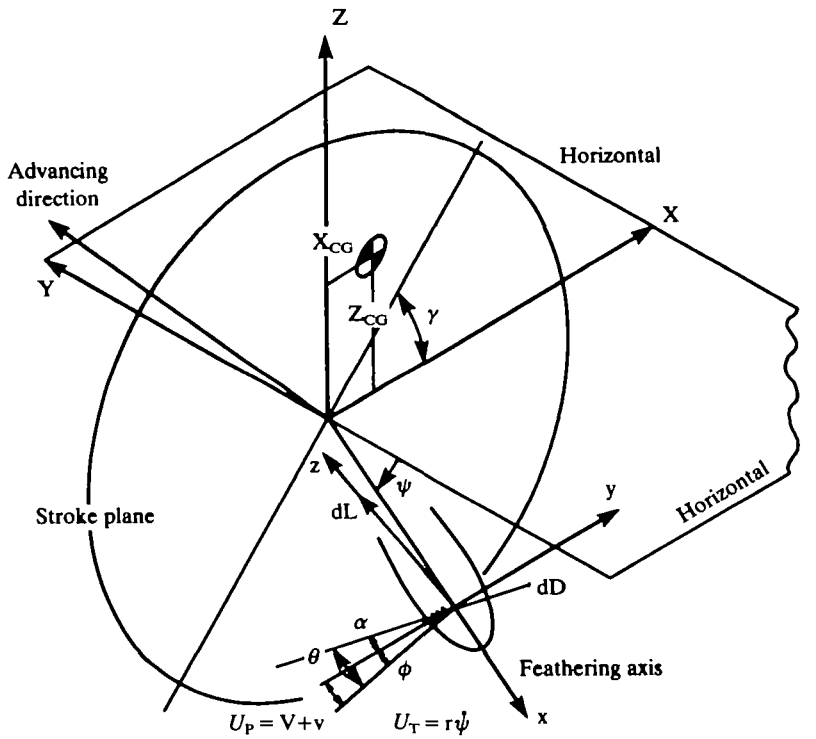

Fig. 7. Coordinate systems related to the beating motion of a wing.

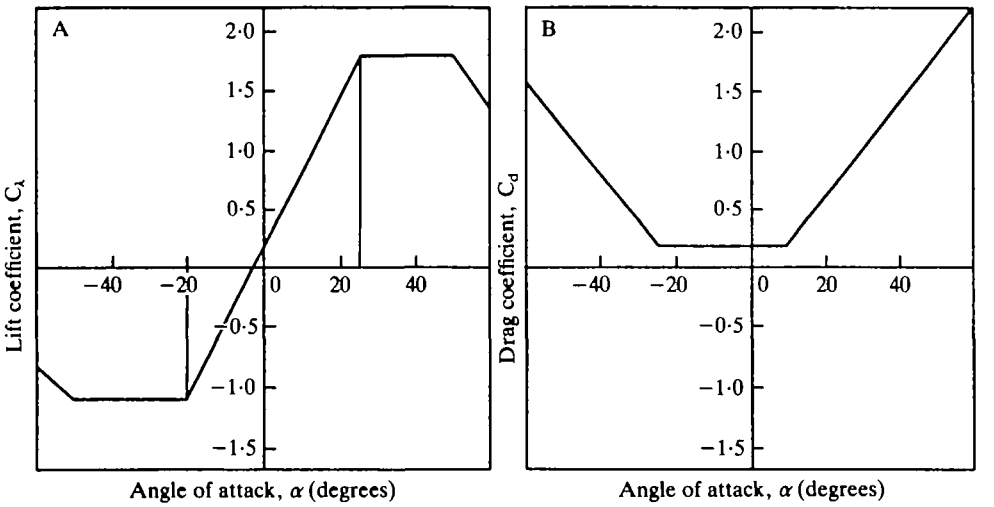

Fig. 8. Assumed aerodynamic characteristics of an airfoil: (A) lift, (B) drag.

considering the effects of the unsteady separated flow and of the dynamic stall on the maximum lift, as presented, for example, by Izumi & Kuwahara (1983), Conner, Willey & Twomey (1965) and Ericsson & Reding (1971).

Referring to Fig. 9A,B, which shows the geometrical relationships about the wing stroke plane, the relative velocities and the aerodynamic forces of the wing for down- and up-strokes respectively, the tangential and perpendicular velocity components, U_T and U_P, are given by:

$$\left.\begin{aligned} U_T &= r\dot{\psi} \\ U_P &= V + v, \end{aligned}\right\} \tag{6}$$

where

$$\left.\begin{aligned} \psi &= \psi_0 + \psi_1 \cos(\omega t + \delta_1) \\ \dot{\psi} &= -\psi_1 \omega \sin(\omega t + \delta_1). \end{aligned}\right\} \tag{7}$$

Then, the elemental lift and drag can be given by

$$\left.\begin{aligned} dL &= \tfrac{1}{2}\rho U^2 c C_\lambda(\alpha) dr \\ dD &= \tfrac{1}{2}\rho U^2 c C_d(\alpha) dr, \end{aligned}\right\} \tag{8}$$

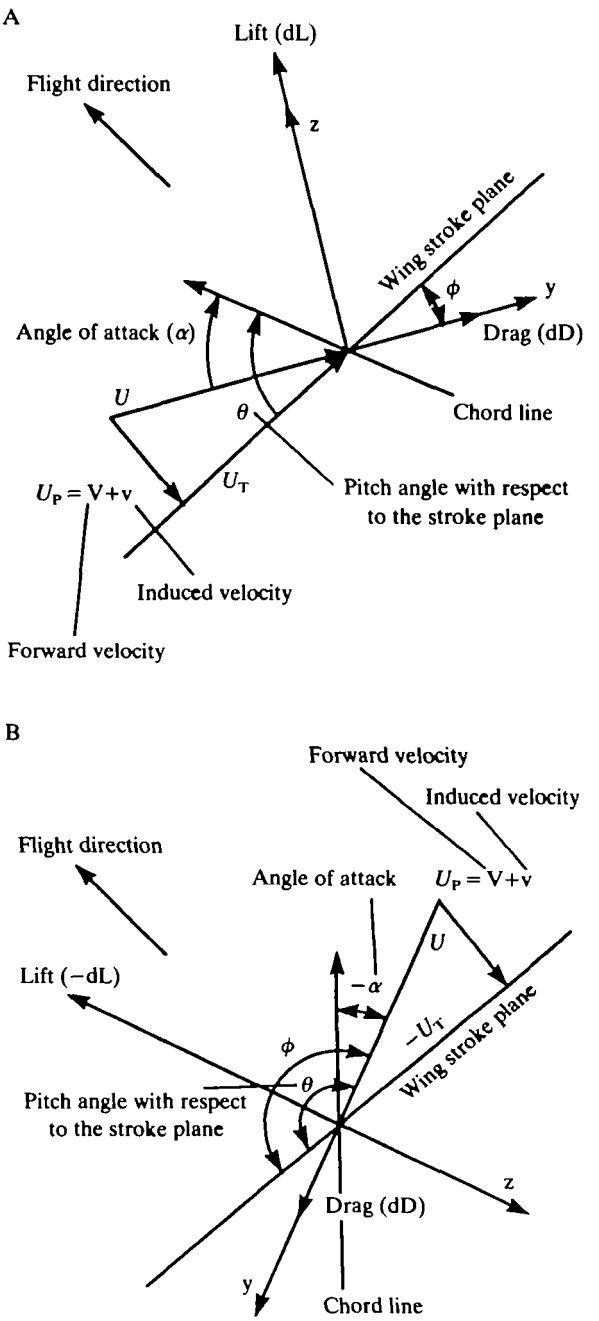

Fig. 9. Relative velocities and aerodynamic forces acting on a blade element. (A) Downstroke; (B) upstroke.

where the relative speed U, the angle of attack α, and the inflow angle ϕ are respectively given by:

$$U = \sqrt{U_T{}^2 + U_P{}^2} = \sqrt{(r\dot{\psi})^2 + (V + v)^2} \tag{9}$$

$$\left.\begin{aligned} \alpha &= \theta - \phi \\ \phi &= \tan^{-1}(U_P/U_T). \end{aligned}\right\} \tag{10}$$

Since the lift and drag of the wing element are directed to the z- and y-axes respectively, the total forces of one pair of wings along the X- and Z-axes and torque, Q, about the joint (positive for flapping up) can respectively be given by:

$$\left.\begin{aligned} F_X &= 2\int \{dD(\cos\psi\cos\phi\cos\gamma + \sin\phi\sin\gamma) + dL(\cos\psi\sin\phi\cos\gamma - \cos\phi\sin\gamma)\} \\ F_Z &= 2\int \{dD(\cos\psi\cos\phi\sin\gamma - \sin\phi\cos\gamma) + dL(\cos\psi\sin\phi\sin\gamma + \cos\phi\cos\gamma)\} \\ Q &= 2\int \{dD\cos\phi + dL\sin\phi\}r. \end{aligned}\right\} \tag{11}$$

Similarly, the thrust, T, pitching moment (head-up positive), M, and the required aerodynamic power, P, are respectively given by:

$$\left.\begin{aligned} T &= F_Z\cos\gamma - F_X\sin\gamma = 2\int (dL\cos\phi - dD\sin\phi) \\ &= \rho\int_0^R V^2 c\{C_\lambda\cos\phi - C_d\sin\phi\}dr \end{aligned}\right\} \tag{13}$$

$$\left.\begin{aligned} M &= F_Z x_{CG} - F_x z_{CG} \\ &= \rho\int_0^R U^2 c[x_{CG}\{C_d(\cos\psi\cos\phi\sin\gamma - \sin\phi\cos\gamma) \\ &\quad + C_\lambda(\cos\psi\sin\phi\sin\gamma + \cos\phi\cos\gamma)\} \\ &\quad - z_{CG}\{C_d(\cos\psi\cos\phi\cos\gamma + \sin\phi\sin\gamma) \\ &\quad + C_\lambda(\cos\psi\sin\phi\cos\gamma - \cos\phi\sin\gamma)\}]dr \end{aligned}\right\} \tag{14}$$

$$\left.\begin{aligned} P &= Q\dot{\psi} = 2\int (dL\sin\phi + dD\cos\phi)r\dot{\psi} \\ &= \rho\int_0^R U^2 c\{C_\lambda\sin\phi + C_d\cos\phi\}\{-\psi_1\omega\sin(\omega t + \delta_1)\}r dr, \end{aligned}\right\} \tag{15}$$

where the aerodynamic power for feathering motion, being very small, is neglected.

The mean values of these quantities during one stroke of beat are, given by:

$$(\bar{\ }) = (\omega/2\pi)\int_0^{2\pi/\omega} (\quad)\mathrm{d}t. \tag{16}$$

By adding the subscripts f and h, the above quantities become those for the fore and hind pairs of wings respectively. For a trimmed steady flight, (i) the mean horizontal force must be balanced by the horizontal component of the parasite drag of the body, which is a very small value or almost zero in the present example,

$$2\bar{F}_X \simeq 0, \tag{17}$$

(ii) the mean vertical force must be balanced with the weight minus the vertical component of the parasite drag which is, however, assumed to be negligibly small and thus, as stated before,

$$2\bar{F}_Z \simeq W \text{ or } \bar{T}_f = \bar{T}_h \simeq W/2\cos\gamma, \tag{18}$$

and the total moment must, by neglecting that produced by the aerodynamic force of the body of the dragonfly, be zero or

$$\bar{M}_f + \bar{M}_h = \bar{M} = 0. \tag{19}$$

By selecting an adequate value of the interference coefficient the above trimmed equations can be satisfied simultaneously. This value was $C_{hf} \simeq 0{\cdot}3$ for $2\bar{F}_2 = W = 2{\cdot}60 \times 10^{-4}$ kgf $= 2{\cdot}54 \times 10^{-3}$ N, and was very much smaller than that expected. In the momentum theory for an isolated single wing the induced velocity must be twice that at the stroke plane in the fully developed wake (Gessow & Myers, 1952). This is probably because the simple analysis, based on the momentum theory and blade element theory is inadequate.

LOCAL CIRCULATION METHOD (LCM)

Since this method is fully described in a paper presented by Azuma *et al.* (1981), only a brief explanation of the method of calculation and the modification made in this method for the beating wing will be presented here.

As shown in Fig. 10, a beating wing can be decomposed into n imaginary wings arranged one-sidedly in diminishing size of span, each of which has an elliptical circulation distribution and thus may be called an elliptical wing, and operates in a twisted flow. Fig. 11 illustrates the flow profile at an arbitrary section as a control point of the flow. Since longitudinal vortex filaments trailing from an elliptical wing do not lie on a flat plate, the induced velocities at that section caused by the respective vortex filaments consequently do not point in the same direction either.

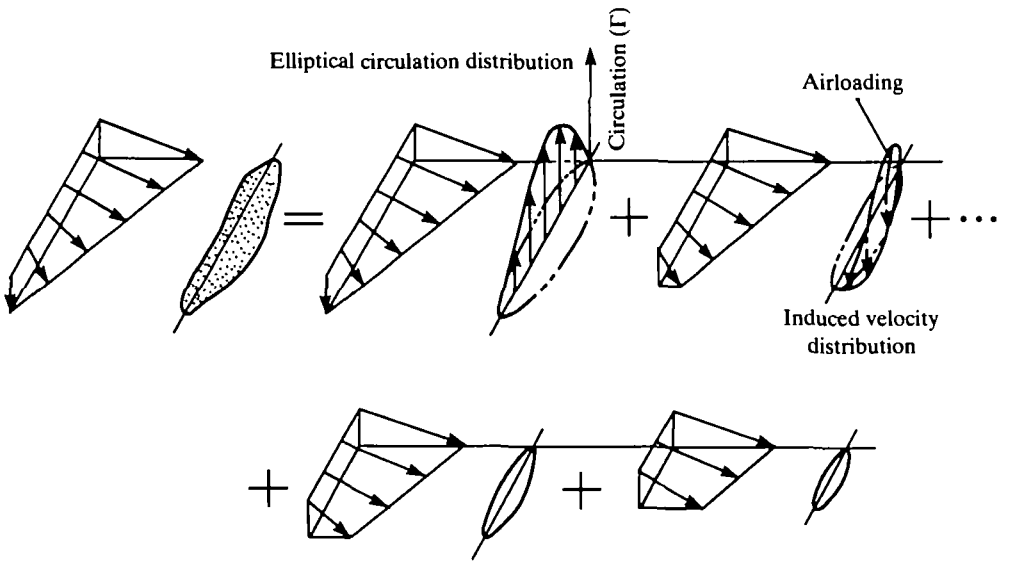

Fig. 10. Decomposition of a beating wing into n wings each having an elliptical distribution of circulation.

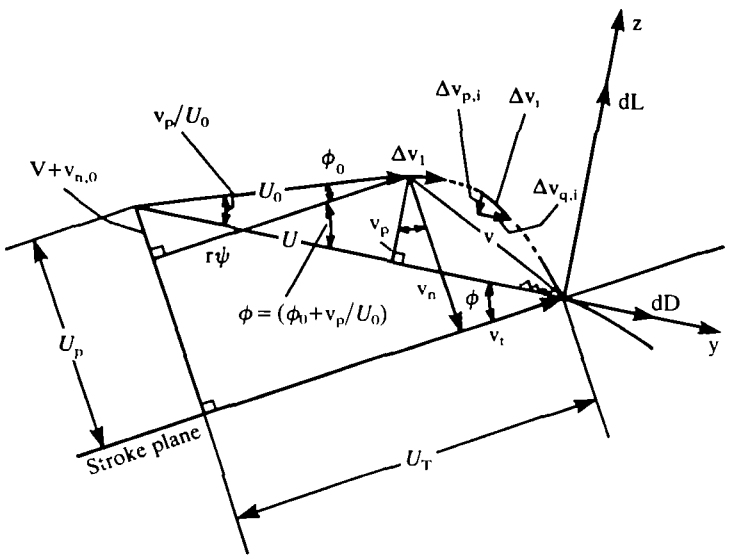

Fig. 11. Relative velocities and forces acting on a blade element at a control point.

By adopting the Kutta-Jukowsky theorem and the blade element theory, the airloading, l, the circulation, Γ, and the lift coefficient as a function of angle of attack $C_\lambda(\alpha)$ can be related as follows:

$$l = \rho \Gamma U \times \mathbf{s} \tag{20}$$

$$= \frac{1}{2} \rho U c C_\lambda(\alpha) U \times \mathbf{s} \tag{21}$$

$$\Gamma = \sum_{i=1}^{n} \Delta\Gamma_i, \tag{22}$$

where $\mathbf{s}$ is a spanwise unit vector. The angle of attack α is, here, considered to be given by:

$$\left.\begin{aligned} \alpha &= \theta - \phi \\ \phi &= \tan^{-1}(U_P/U_T), \end{aligned}\right\} \tag{23}$$

where U_T and U_P are respectively tangential and perpendicular components of the total inflow velocity U, with respect to a stroke plane, at a control point under consideration.

Referring to Fig. 11, the perpendicular and tangential components of the induced velocity with respect to the total inflow U can be given by the summation of the components induced by the respective wings,

$$\left.\begin{aligned} v_p &= \sum_{i=1}^{n} \Delta v_{p,i} \\ v_q &= \sum_{i=1}^{n} \Delta v_{q,i} \end{aligned}\right\} \tag{24}$$

and are related to the circulation $\Delta\Gamma_i$ as follows:

$$\left.\begin{aligned} \Delta v_{p,i} &= \frac{1}{4\pi} \int_0^R \frac{\cos\{\phi(r') - \phi(r_i)\}}{r_i - r'} \frac{d\Delta\Gamma_i(r')}{dr'} dr' \\ \Delta v_{q,i} &= \frac{1}{4\pi} \int_0^R \frac{\sin\{\phi(r') - \phi(r_i)\}}{r_i - r'} \frac{d\Delta\Gamma_i(r')}{dr'} dr'. \end{aligned}\right\} \tag{25}$$

Then, the tangential and normal components of the induced velocity and of the total inflow velocity with respect to the stroke plane can be given by:

$$\left.\begin{aligned} v_t &= -v_p \sin\phi + v_q \cos\phi \\ v_n &= v_p \cos\phi + v_q \sin\phi \end{aligned}\right\} \tag{26}$$

$$\left.\begin{aligned} U_T &= r\psi + v_t \\ U_P &= V + v_{n,0} + v_n, \end{aligned}\right\} \tag{27}$$

where $v_{n,0}$ is the normal component of the induced velocity with respect to the stroke plane, generated and left by the preceding wings at the control point, whereas v_n is that generated by the present wing at the present time.

If the induced velocity left on the control point, $V_{n,0}$, is specified as a known value or related to other known variables, then by combining equations (20) to (27), the spanwise distribution of the airloading, circulation and the perpendicular and tangential components of the induced velocity can be solved numerically. If the induced velocity outside the elliptical wings is neglected, then the solution can be obtained successively (Azuma & Kawachi, 1979).

Now let us consider the induced velocity $v_{n,0}$. In the local circulation method for a rotary wing (Azuma *et al.* 1981) the induced velocity left at the control point at time step t_{j-1} is considered to be given by multiplying the induced velocity generated at the control point at a time t_{j-1}, v^{j-1}, by an attenuation coefficient C^{j-1} as $C^{j-1}v^{j-1}$. In the case of two pairs of wings, the induced velocities left at the control points (P_f and P_h) for the fore and hind pairs of wings, can respectively be given by:

$$\left.\begin{aligned} (v_{n,0})_f^j &= C_f^{j-1}\,(v_f^{j-1} + C_{fh} v_h^{j-1}) \\ (v_{n,0})_h^j &= C_h^{j-1}\,(v_h^{j-1} + C_{hf} v_f^{j-1}), \end{aligned}\right\} \tag{28}$$

where v_f^{j-1} and v_h^{j-1} are respectively the induced velocities of the fore and hind pairs of wings at the control points at the time t_{j-1}, and where C_f^{j-1}, C_h^{j-1} and C_{fh}, C_{hf} are direct or time-related attenuation coefficients and cross- or space-related interference coefficients respectively.

By referring to Fig. 12A,B, the interference coefficients C_{fh} and C_{hf} may be given by the ratio of the induced velocity generated by the respective system of trailing vortex as follows:

$$\left.\begin{aligned} C_{hf} &= (v_{P_h}/v_{P_f})_f \\ C_{fh} &= (v_{P_f}/v_{P_h})_h, \end{aligned}\right\} \tag{29}$$

where $(\ )_f$ and $(\ )_h$ show the quantity $(\ )$ specified by the trailing vortex of the fore and hind wings, respectively. Since the effect of shed vortices on the downwash at the most active part of the respective wing, i.e. at spanwise position of $r = (3/4)R$ and azimuth angle of $\psi = 0°$, can be neglected in comparison with that of the trailing vortex, only the trailing vortex has been considerated for the determination of the interference coefficients and the attenuation coefficients. Usually, C_{fh} can further be neglected as being a small quantity (Azuma & Saito, 1979).

Then, by referring to Fig. 13A,B, the attenuation coefficients C_f and C_h may be given by the ratio of the induced velocities generated by the trailing vortices of both pairs of wings at time t_j and $t_j + \Delta t$ as follows:

$$\left.\begin{aligned} C_f^j &= v_{P_f}(t_j + \Delta t)/v_{P_f}(t_j) \\ C_h^j &= v_{P_h}(t_j + \Delta t)/v_{P_h}(t_j). \end{aligned}\right\} \tag{30}$$

In the determination of the interference and attenuation coefficients, the trailing vortices are considered to be tip vortices generated by each wing and clinging around a

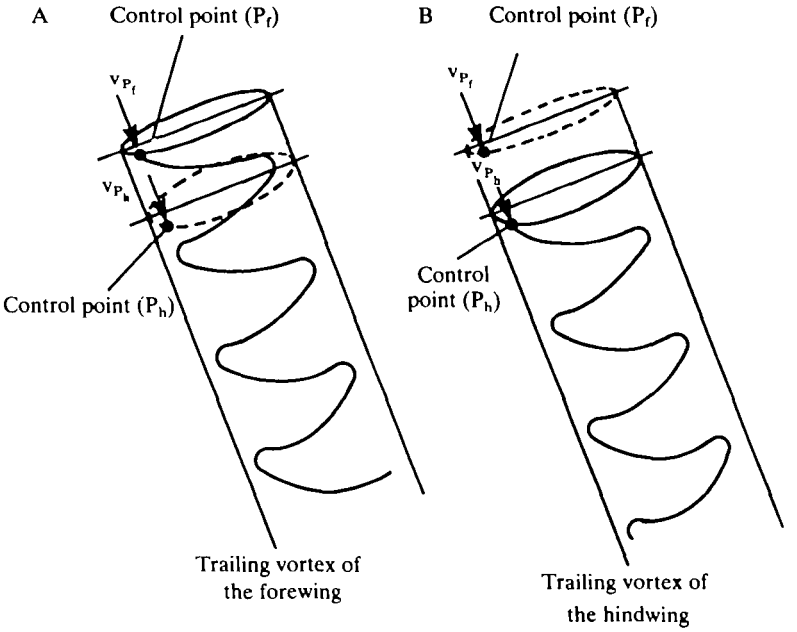

Fig. 12. Induced velocities for determining the interference coefficients. (A) Induced velocity generated by the trailing cortex of forewing; (B) induced velocity generated by the trailing vortex of hindwing.

wake cylinder as shown in Fig. 14. The respective vortex systems are assumed to flow downstream with a constant flow speed $\bar{U}_P$ which is the mean value of the normal flow U_P or:

$$\bar{U}_P = \frac{1}{S}\int U_P dS, \tag{31}$$

where S is the area of the respective stroke plane.

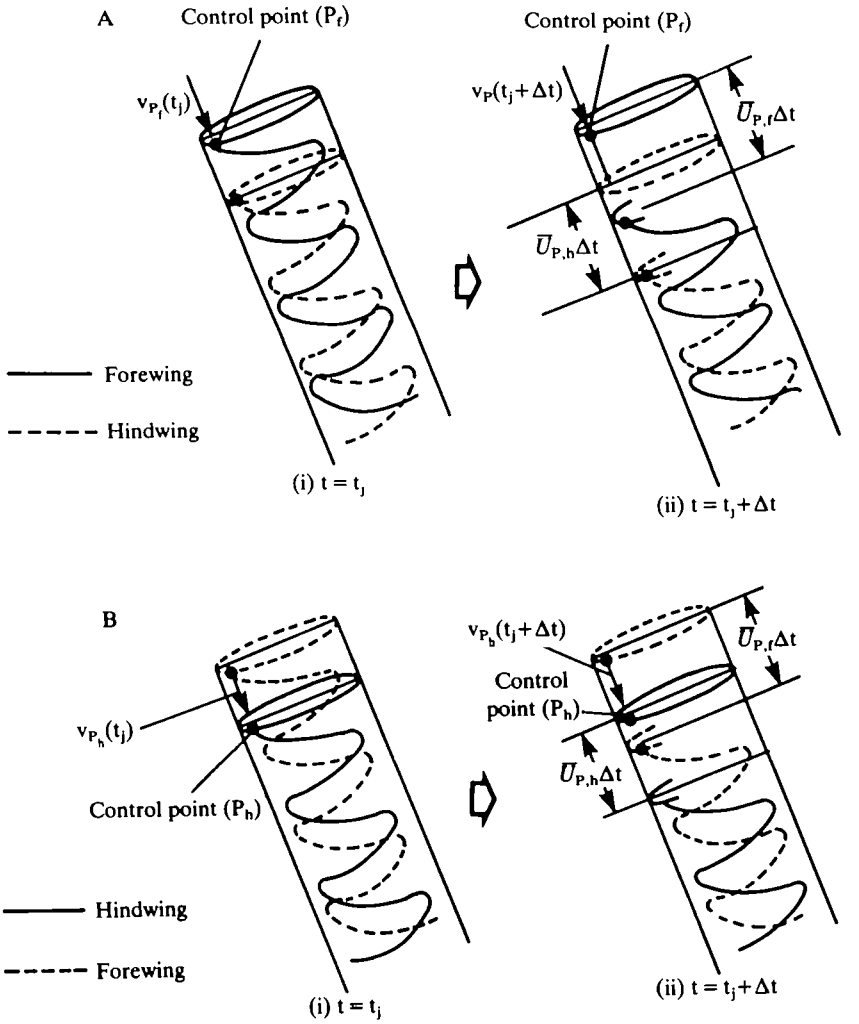

Fig. 13. Induced velocities for determining the attenuation coefficients. (A) Forewing; (B) hindwing.

The positions of the control point P and the element Q of the tip vortices of the respective pairs of wings in a polar coordinate system can be given by:

$$\left.\begin{aligned} r_P &= R \\ \psi_P &= \psi_0 + \psi_1 \cos\delta_1 \\ \zeta_P &= 0 \end{aligned}\right\} \tag{32}$$

and

$$\left.\begin{aligned} r_Q &= R \\ \psi_Q &= \psi_0 + \psi_1 \cos(\omega t + \delta_1) \\ \zeta_Q &= \bar{U}_P \cdot t. \end{aligned}\right\} \tag{33}$$

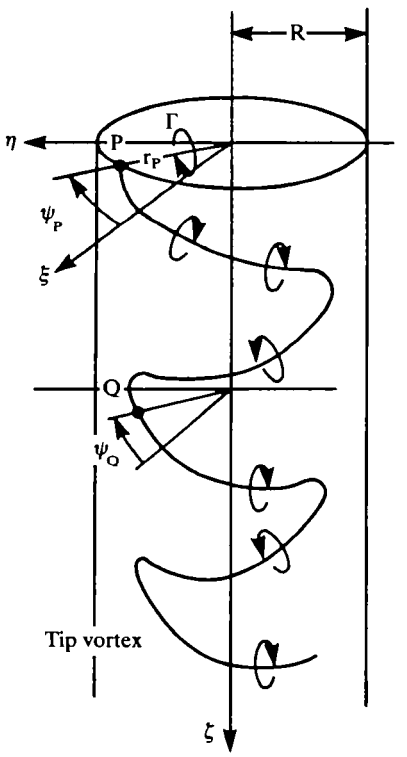

Fig. 14. Trailing and shed vortex model for determination of the interference and of the attenuation coefficient.

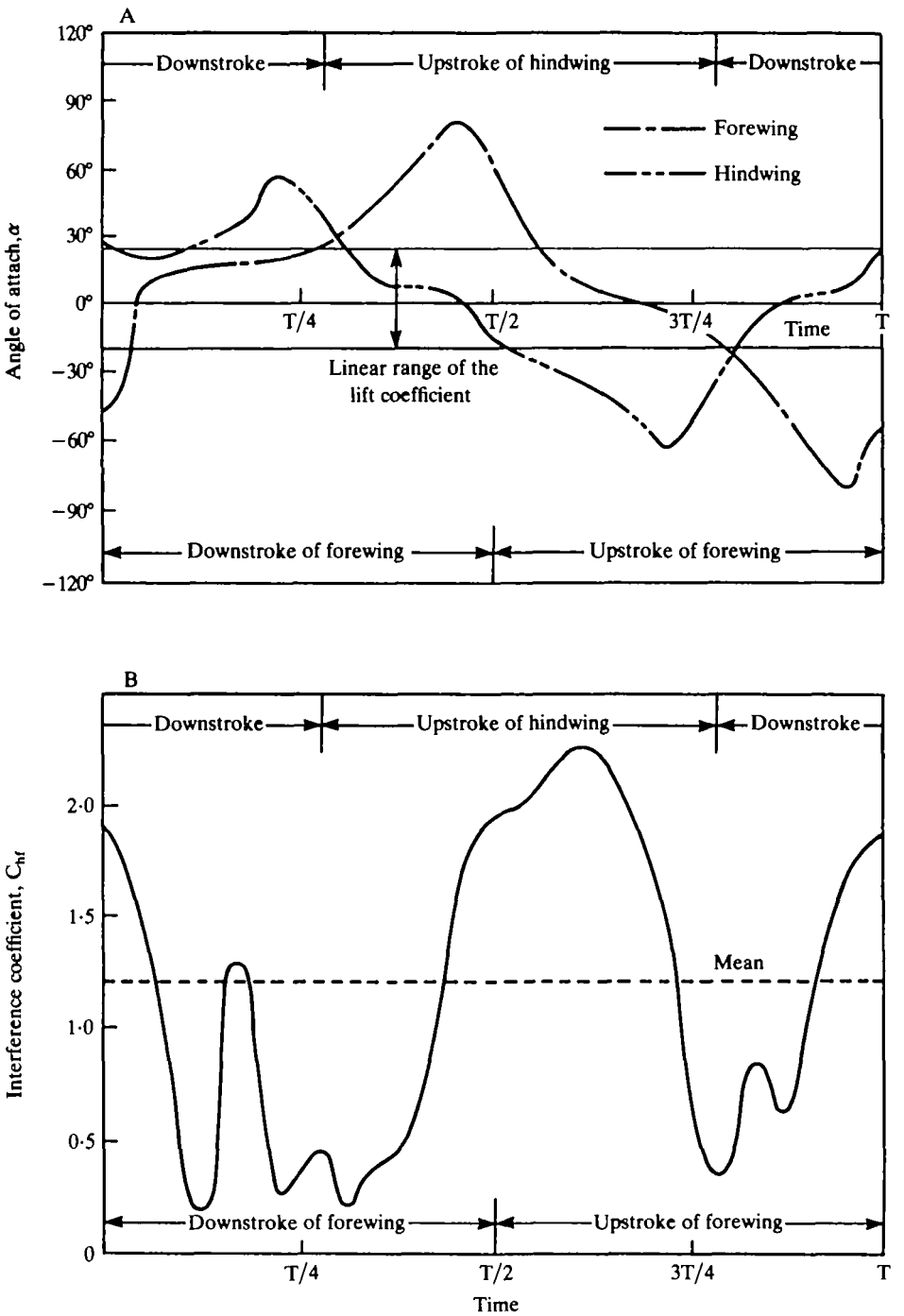

Fig. 15. Time variation of flow at $r = 0{\cdot}75R$. (A) Angle of attack; (B) interference coefficient.

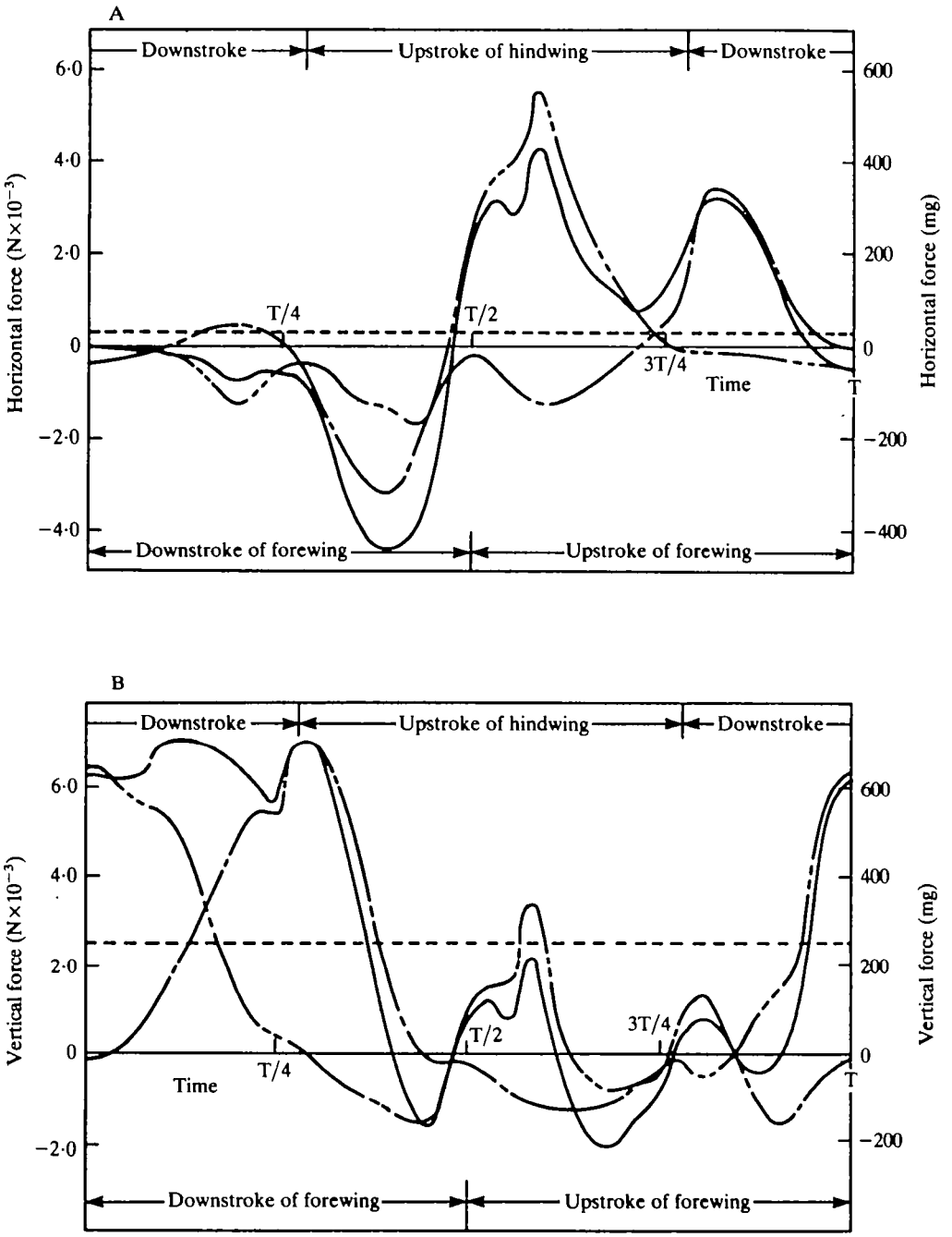

Fig. 16. Time variations of forces, moment and power. (A) Thrust, (B) vertical force, (C) pitching moment, (D) power. (———) Forewing; (— — —) hindwing; (——) resultant, (– – –) mean.

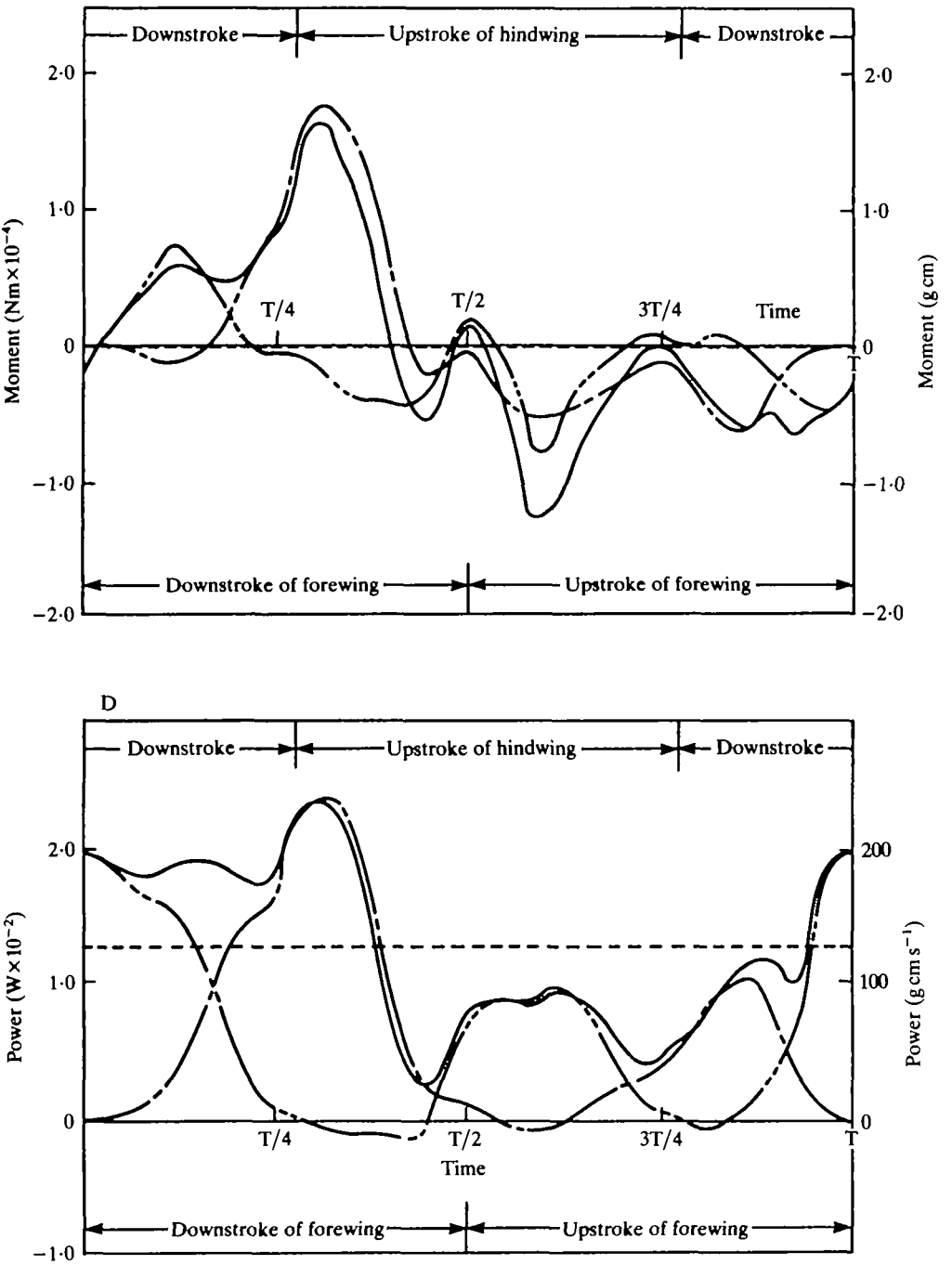
Downstroke
Upstroke of hindwing
Downstroke
2·0
1·0
0
−1·0
−2·0
Moment (Nm×10⁻⁴)
T/4
T/2
3T/4
Time
T
Moment (g cm)
Downstroke of forewing
Upstroke of forewing
D
Power (W×10⁻²)
200
100
Power (g cm s⁻¹)

Fig. 16C,D

Then, by applying Biot-Savart's law, the induced velocity at the control point, P, is determined by:

$$v_P = -\frac{1}{4\pi}\int_{-\infty}^{0} \Gamma(t)\cdot\frac{dr_Q \times a}{|a|^3}, \tag{34}$$

where

$$a = r_P - r_Q \tag{35}$$

and the circulation $\Gamma(t)$ is assumed to be represented at the three-quarter radius point, $r = 0{\cdot}75R$.

$$\Gamma(t) = \frac{1}{2}\{cUC_\lambda(\alpha)\}_{r=0{\cdot}75R}. \tag{36}$$

By introducing iterative calculation, these equations can be used to determine the induced velocity distribution $v_{n,0}$ at time t_j for both the fore and hind pairs of wings successively.

Since the aerodynamic forces along z- and y-axis components can again be given by:

$$\begin{aligned} dL &= \lambda dr = \rho\Gamma U dr \\ dD &= \frac{1}{2}\rho U^2 c C_d, \end{aligned} \tag{37}$$

the total forces and moments generated by the respective pair of wings can be obtained from equations (11) to (16).

RESULTS CALCULATED BY THE LCM

By applying the LCM for a steady, slow-climbing flight of a dragonfly and by using the observed data, the following results have been obtained.

The time variations of the angle of attack α, and the interference coefficient C_{hf} at the three-quarter radius point of the wing for the fore and hind pairs are shown in Fig. 15. It is remarkable that the angles of attack remain in the linear range of the lift coefficient during the effective phase of the respective strokes and the interference coefficient varies appreciably. The C_{hf} is less effective near the switching of the beating strokes of the hindwings, from up to down and down to up, where the induced velocity generated by the forewing is predominant. This results from adequate selection of the phase lead of the hindwing $\delta_1 = 77°$. The mean value of the interference coefficient is about $C_{hf} = 1{\cdot}2$, which is more reasonable and much larger than that given in the Simple Analysis section (p. 88).

Fig. 16 shows the time variations of the horizontal force, vertical force, pitching moment and power. The negative horizontal force is generated mainly by the forewing in the latter half of its downstroke, whereas the positive horizontal force is generated by the hindwing in the last half of its upstroke. The mean horizontal force is a very small positive value because the dragonfly is climbing only slowly.

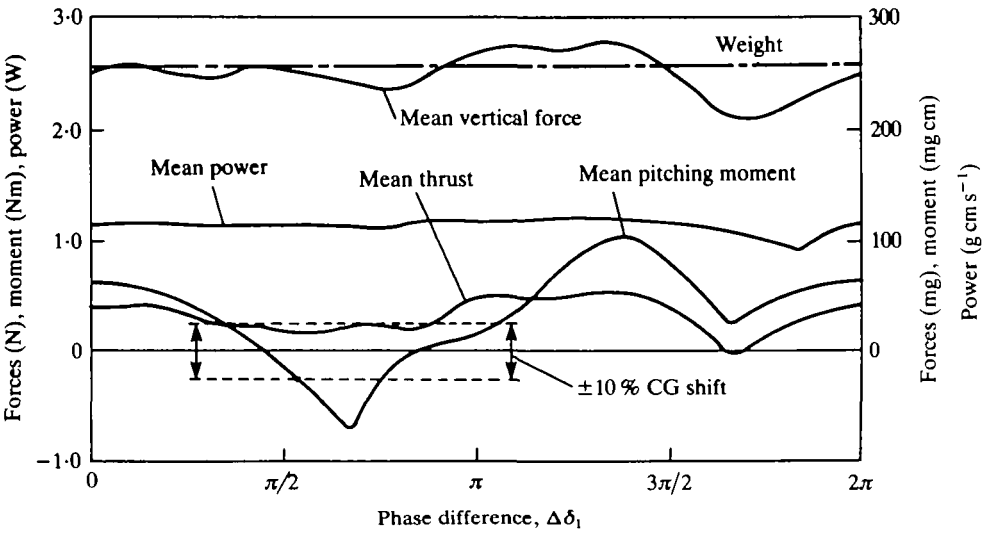

Fig. 17. Effect of the phase differences of the mean vertical force ($2\bar{F}_z \times 10^3$, N), mean horizontal force ($2\bar{F}_x \times 10^3$, N), mean pitching moment ($\bar{M} \times 10^7$, Nm) and mean power ($\bar{P} \times 10^2$, W).

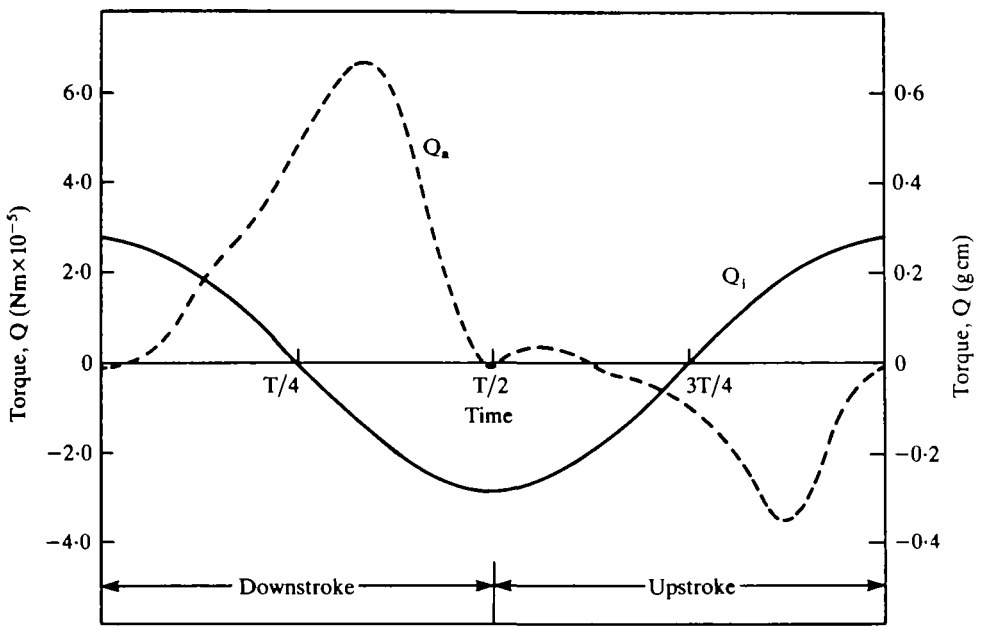

Fig. 18. Time variation of the torque of a forewing. Q_i, inertia torque; Q_a, aerodynamic torque.

The vertical force is mostly generated in the downstroke of the respective wings. The total mean vertical force is equal to the weight of the dragonfly. The higher harmonics of pitch changes are important to keep this balance.

The moment about the centre of gravity, which was not always accurately observed but only roughly measured, varies appreciably during the wing cycle, from positive in the downstroke of the forewing to negative in the upstroke of the forewing. The mean value is, however, almost zero for a steady flight.

The power is always positive and its variation is very similar to that of the vertical force. That is to say, the power is mainly consumed to sustain the weight of the body in this example. The mean value of this required power is equivalent to a 'specific power' of 160 W kg^{-1}, which is the required power per unit mass of muscle. This value falls in a reasonable range (70–260 W kg^{-1}) as estimated by Weis-Fogh (1975, 1977).

The effects of the phase difference $\Delta\delta_1$ of the beating motion between the fore and hind pairs of wings on the mean values of horizontal force, vertical force, pitching moment and power are shown in Fig. 17. The horizontal force and pitching moment are strongly dependent on the phase difference or phase lead of the hindwing δ_1, whereas the vertical force and power are almost invariant or slightly dependent on the phase difference. There are two phase differences for zero pitching moment, $\Delta\delta_1 = 80°$ and 150°. As shown by dotted lines in Fig. 17, by adjusting the CG position from -10% (forward) to $+10\%$ (backward) of the mean wing chord the above trimmed phase difference varies as $60° < \Delta\delta_1 < 95°$ and $140° < \Delta\delta_1 < 190°$. The former phase difference gives a small mean horizontal force for low-speed flight whereas the latter one generates a large mean horizontal force probably for high-speed flight. The observed value of $\Delta\delta_1 \simeq 80°$ clearly corresponds to the above low-speed flight. Contrary to expectation, the power was not small at the former trimmed point.

In the above calculations, the unsteady flow effects on the aerodynamic forces and moments acting on the beating wings have not been introduced. In the linear unsteady wing theory the effects of periodically shed vortices are introduced by simply multiplying either the Theodorsen function for the wing motion or the Sear's function for the change of oncoming flow by the lift slope as precisely explained in textbooks (e.g. Bisplinghoff, Ashley & Halfman, 1955). In the present calculation, however, the effects of shed vortices have been introduced as the spanwise variation of the induced velocity generated and left by the preceding blades by the term of $(v_{n,0})^{j}_{f \text{ or } h}$ as given by equation (31). Since the chordwise gradient of this term is nearly equivalent to the shed vortices (Azuma *et al.* 1982), other unsteady effects have been omitted.

CONTRIBUTION OF INERTIAL FORCE

The inertial force accompanying the beating motion results mainly from the flapping motion in the stroke plane. The inertial torque of a single wing assumed to be rigid can be given by:

$$Q_i = \int_0^R \ddot{\psi}(\mathrm{d}m/\mathrm{d}r)\mathrm{d}r = I\ddot{\psi}, \tag{38}$$

where I is the inertial moment about the flapping hinge. By assuming the wing to be a thin rectangular plate, this inertial moment is estimated as $I = 5{\cdot}5 \times 10^{-11}\,\mathrm{kg\,s^{-2}}$.

Shown in Fig. 18 are the time variations in the inertial torque Q_i and the aerodynamic torque Q_a of a forewing beating in the same steady flight. In the latter half of both the down- and upstrokes the inertial torque assists to compensate the aerodynamic torque. It is, however, known that the inertial torque can be cancelled or reduced by adopting either an elastic property into the wing itself or a resilient material such as an apodeme at the flapping hinge of the wing (Weis-Fogh, 1972; Alexander, 1975).

REFERENCES

ALEXANDER, R. M. (1975). *Biomechanics*. London: Chapman & Hall Ltd. New York: Halsted Press.

AZUMA, A., HAYASHI, T. & ITO, A. (1982). Application of the local circulation method to the flutter analysis of rotary wings. Eighth European Rotorcraft and Powered lift Aircraft Forum.

AZUMA, A. & KAWACHI, K. (1979). Local momentum theory and its application to the rotary wing. *J. Aircraft* **16**, 6–14.

AZUMA, A., NASU, K. & HAYASHI, T. (1981). An extension of the local momentum theory to the rotors operating in twisted flow field. *Vertica* **7**, 45–59.

AZUMA, A. & SAITO, S. (1979). Application of the local momentum theory to the aerodynamic characteristics of multi-rotor systems. *Vertica* **3**, 131–144.

AZUMA, A. & SAITO, S. (1982). Study of rotor gust response by means of the local momentum theory. *J. Am. Helicopter Soc.* **27**, 58–72.

BISPLINGHOFF, R. L., ASHLEY, H. & HALFMAN, R. L. (1955). *Aeroelasticity*. Reading, MA: Addison-Wesley Publishing Co. Inc.

CONNER, F., WILLEY, C. & TWOMEY, W. (1965). A flight and wind tunnel investigation of the effect of angle-of-attack rate on maximum lift coefficient. *NASA CR*-**321**.

ERICSSON, L. E. & REDING, J. P. (1971). Unsteady airfoil stall, review and extension. *J. Aircraft* **8**, 609–616.

GESSOW, A. & MYERS, G. C., JR. (1952). *Aerodynamics of the Helicopter*. New York: Macmillan Publishing Company.

HEYSON, H. H. & KATZOFF, S. (1957). Induced velocities near a lifting rotor with nonuniform disc loading. *NACA Rep.* **1319**.

ISHIDA, S. (1980). *Insects' Life in Japan*, Vol. 2, *Dragonflies*. Tokyo: Hoikusha Publishing Co. Ltd.

IZUMI, K. & KUWAHARA, K. (1983). Unsteady flow field, lift and drag measurements of impulsively started elliptic cylinder and circular-arc airfoil. AIAA 16th Fluid and Plasma Dynamics Conference, Danvers, MA U.S.A., July 12–14.

JENSEN, M. (1956). Biology and physics of locust flight. III. The aerodynamics of locust flight. *Phil. Trans. R. Soc. Ser. B* **239**, 511–552.

NORBERG, R. ÅKE. (1972). The pterostigma of insect wings: an inertial regulator of wing pitch. *J. comp. Physiol.* **81**, 9–22.

NORBERG, R. ÅKE. (1975). Hovering flight of the dragonfly *Aeschina juncea* L.: kinematics and aerodynamics. In *Swimming and Flying in Nature*, Vol. 2, (eds T. Y.-T. Wu, C. J. Brokaw & C. Brennen), pp. 763–781. New York: Plenum Press.

RAYNER, J. M. V. (1979*a*). A vortex theory of animal flight. I. The vortex wake of a hovering animal. *J. Fluid Mech.* **91**, 697–730.

RAYNER, J. M. V. (1979*b*). A vortex theory of animal flight. II. The forward flight of birds. *J. Fluid Mech.* **91**, 731–763.

RAYNER, J. M. V. (1979*c*). A new approach to animal flight mechanics. *J. exp. Biol.* **80**, 17–54.

VOGEL, S. (1967). Flight in *Drosophila*. III. Aerodynamic characteristics of fly wings and wing models. *J. exp. Biol.* **46**, 413–443.

WEIS-FOGH, T. (1972). Energetics of hovering flight in hummingbirds and in *Drosophila*. *J. exp. Biol.* **56**, 79–104.

WEIS-FOGH, T. (1975). Flapping flight and power in birds and insects, conventional and novel mechanisms. In *Swimming and Flying in Nature*, Vol. 2, (eds T. Y.-T. Wu, C. J. Brokaw & C. Brennen), pp. 729–762. New York: Plenum Press.

WEIS-FOGH, T. (1977). Dimensional analysis of hovering flight. In *Scale Effects in Animal Locomotion*. London: Academic Press.